

Modeling of the lamellar structure of ethylene-1-octene copolymers^{*})

Stanisław Rabiej^{1), **)}, Małgorzata Rabiej¹⁾

DOI: [dx.doi.org/10.14314/polimery.2014.549](https://doi.org/10.14314/polimery.2014.549)

Abstract: The parameters of the lamellar structure of melt crystallized ethylene-1-octene copolymers were determined with the usage of model calculations. Two models were employed: classical model of Hosemann and a variable local structure model. In the second model it was assumed that the crystallinity of stacks varies from stack to stack according to some distribution function $P(\varphi)$. Theoretical SAXS curves related to the assumed models were best fitted to the experimental curves and the parameters of stacks were determined. It was found that the second model gave much better fits than the model of Hosemann. Generally, the distribution function $P(\varphi)$ is asymmetric and positively skewed but its shape changes for the stacks crystallized at various temperatures. At higher temperatures, starting from the melting point, the crystallinity distribution can be well approximated by the Reinhold function. At lower temperatures, closer to the final solidification, the split Gauss function is a better approximation.

Keywords: SAXS, modeling, lamellar structure, crystallinity, distribution function.

Modelowanie struktury lamelarniej kopolimerów etylen-1-okten

Streszczenie: Badano strukturę lamelarną kopolimerów etylen-1-okten podczas ich chłodzenia od temperatury topnienia do temperatury pokojowej. Parametry struktury wyznaczano na podstawie obliczeń modelowych, polegających na optymalnym dopasowywaniu teoretycznej krzywej rozpraszania SAXS, odpowiadającej założonemu modelowi struktury, do krzywej eksperymentalnej. W obliczeniach stosowano klasyczny model Hosemanna, zgodnie z którym wszystkie stosy lamelarne występujące w polimerze są statystycznie identyczne, oraz model zakładający niejednorodność struktury polimeru. Ten ostatni model zakładał, że stopień krystaliczności stosów jest zróżnicowany, a jego występowanie w objętości polimeru opisuje pewna funkcja rozkładu $P(\varphi)$. Badania wykazały, że nie jest możliwe uzyskanie dobrego dopasowania krzywych teoretycznych, opisanych zależnościami podanymi przez Hosemanna, do krzywych eksperymentalnych, co tym samym świadczy o nieadekwatności tego modelu w odniesieniu do badanych struktur. Zastosowanie drugiego modelu pozwoliło na uzyskanie bardzo dobrego dopasowania w całym zakresie rejestracji krzywych SAXS. Otrzymane wyniki świadczą o niejednorodnej strukturze stosów lamelarnych w badanych kopolimerach oraz o asymetrycznym charakterze rozkładu stopnia krystaliczności w stosach. W zakresie wysokich wartości temperatury, rozkład ten może być bardzo dobrze opisany za pomocą funkcji Reinholda. W zakresie niższych wartości temperatury, bliskich temperaturze końcowego zestalenia się kopolimeru, lepszym przybliżeniem jest tzw. składowa funkcja Gaussa.

Słowa kluczowe: SAXS, modelowanie, struktura lamelarna, krystaliczność, funkcja rozkładu.

The parameters of lamellar structure of semicrystalline polymers (like the average long period, average thicknesses of crystalline lamellae and amorphous layers, volume crystallinity etc.) can be determined based on the one-dimensional correlation function $K(x)$, obtained by Fourier transformation of experimental SAXS curve,

using the methods developed by Vonk [1] and Strobl [2]. Alternatively, the parameters can be determined by model calculations which consist in construction of a theoretical scattered intensity function related to the assumed model of a polymer structure and best fitting of this theoretical function to the experimental SAXS curve. Reviews and comparisons of existing models one can find in the works of Crist [3] or Stribeck [4]. The most important and generally accepted as the best representation of the lamellar aggregates in polymers is so called *the general paracrystalline* [3] or *the stacking* [4] model. In this model, a polymer volume is considered as an isotropic system of randomly oriented and uniformly distributed stacks. The stacks are composed of flat, lamellar crystals separated

¹⁾ Institute of Textile Engineering and Polymer Materials, University of Bielsko-Biała, Willowa 2, 43-300 Bielsko-Biała, Poland.

^{*}) Material contained in this article was presented at the IX International Conference "X-Ray investigations of polymer structure", Zakopane, Poland, 3–6 December 2013.

^{**)} Corresponding author; e-mail: stanislaw.rabiej@ath.bielsko.pl

by amorphous layers. A single stack is regarded as a disordered one dimensional structure. The thicknesses of crystals and amorphous layers fluctuate independently on one another and they are described by independent distribution functions. The first approach assumes that the stacks are statistically identical in respect of their internal structure. It means that all of them are characterized by the same average values of amorphous layer thickness A_o , average crystalline lamella thickness C_o and average long period L_o , where $L_o = A_o + C_o$. The distributions of the thicknesses of amorphous and crystalline layers in all stacks are described by the same functions $G_1(A)$ and $G_2(C)$. Theoretical intensity function for such a model is expressed by the relationships derived by Hosemann [5]. In the literature one can find several examples of application of various versions of such a model for various polymers [6–10]. These versions differ in the type of distribution functions $G_1(A)$ and $G_2(C)$ (Gauss or others) or in the number of layers in one stack (infinite or some limited number). More complex models assume that the structure of all stacks is not the same i.e. the heterogeneity of a polymer is admitted [9–13]. It means that the thicknesses of the crystalline and amorphous layers fluctuate both within the stacks [depicted by $G_1(A)$ and $G_2(C)$ distributions] as well as between the stacks.

In this work we investigated the lamellar structure of ethylene-1-octene copolymers of moderate (5.5 mol % and 6.6 mol %) concentration of 1-octene, during cooling of the samples from the melt to room temperature. The SAXS curves (total number amounted to 91) were recorded at different stages of crystallization. Owing to this fact we could evaluate the usefulness of various models at various stages. We employed both the model of Hosemann according to which whole polymer can be represented by one stack and so called variable local structure model in which the polymer is inhomogeneous and the scattered intensity is the weighted average of intensities scattered by all stacks. We assumed that the stacks differ in their volume crystallinity which varies from stack to stack according to some distribution function $P(\varphi)$. Calculations were performed for various distribution functions $P(\varphi)$ starting from the Gauss distribution.

Theoretical intensity functions related to the assumed model were best fitted to the experimental curves using, modified module of our computer program SAXSDAT [14] elaborated to this aim. The module has been equipped with several $P(\varphi)$ functions. Finally the parameters of stacks determined from curves fitting method were compared with those found from the correlation function.

MODEL OF HOSEMANN

In the general model of Hosemann [5], the stacks are considered as strictly two phase systems with sharp phase boundaries in which the thicknesses of the crystalline (C) and amorphous (A) layers vary independently of each other according to some distribution functions $G_1(C)$

and $G_2(A)$. The lateral size of stacks is much bigger than the wavelength of X-rays and much bigger than the long period. For this reason, the intensity scattered by the stacks is influenced only by the one-dimensional fluctuation of electron density perpendicular to the lamellar planes. All stacks are statistically identical, so the whole system can be represented by a single stack. According to Hosemann, the one dimensional intensity scattered perpendicularly to the layers of such a stack is a sum of two components:

$$I_1(s) = I_C(s) + I_B(s) \quad (1)$$

where:

$$I_C(s) = \frac{(\Delta\rho)^2}{2\pi^2 s^2 N L_o} \operatorname{Re} \left\{ \frac{F_A(1-F_C)^2 (1-(F_A F_C)^N)}{(1-F_A F_C)^2} \right\} \quad (2)$$

and

$$I_B(s) = \frac{(\Delta\rho)^2}{2\pi^2 s^2 L_o} \operatorname{Re} \left\{ \frac{(1-F_C)(1-F_A)}{(1-F_C F_A)} \right\} \quad (3)$$

$I_C(s)$ is zero order component and $I_B(s)$ is called Babinet component.

In the formulas (2) and (3) $s = 2\sin\theta/\lambda$ is the scattering vector, λ is the wavelength, $\Delta\rho = \rho_1 - \rho_2$ is the electron density difference between the crystalline and amorphous phases, L_o is the average long period, N is the average number of lamellae in one stack and F_C , F_A are Fourier transforms of the thickness distributions of crystalline and amorphous layers $G_1(C)$ and $G_2(A)$.

The zero order component is scattered at very small angles and already for N higher than 20 it is below experimentally accessed range of angles — it is covered by the beam stop [10, 15]. So in practice, the observable intensity profile is described by the Babinet component only. The Babinet component is symmetrical in respect of the crystalline and amorphous phases reflecting the Babinet's principle and it determines the position and shapes of diffraction maxima observed in the scattering curve.

In the calculations described in this paper it is assumed that N is large enough that zero order component $I_C(s)$ can be neglected and $G_1(C)$ and $G_2(A)$ are assumed to be Gauss distributions with the respective standard deviations σ_C and σ_A :

$$G_2(A) = \frac{1}{\sigma_A \sqrt{2\pi}} \exp \left[-\frac{(A - A_o)^2}{2\sigma_A^2} \right] \quad (4)$$

$$G_1(C) = \frac{1}{\sigma_C \sqrt{2\pi}} \exp \left[-\frac{(C - C_o)^2}{2\sigma_C^2} \right]$$

Moreover, because the thicknesses of the crystalline and amorphous layers vary independently of each other, the standard deviation of long period σ_L is equal to:

$$\sigma_L^2 = \sigma_C^2 + \sigma_A^2 \quad (5)$$

Then, the Fourier transforms of $G_1(C)$ and $G_2(A)$ functions are given by:

$$\begin{aligned} F_A &= \exp(-2\pi^2 s^2 \sigma_A^2) \exp(2\pi s i A_o) \\ F_C &= \exp(-2\pi^2 s^2 \sigma_C^2) \exp(2\pi s i C_o) \end{aligned} \quad (6)$$

and the Babinet component takes the shape:

$$I_B(s) = \frac{(\Delta\rho)^2}{2\pi^2 s^2 L_0} \frac{1 - |F_L|^2 - |F_C| \left((1 - |F_A|^2) \cos(2\pi s C_0) - |F_A| \left((1 - |F_C|^2) \cos(2\pi s A_0) \right) \right)}{|1 - F_L|^2} \quad (7)$$

where: $F_L = F_C \cdot F_A = \exp[-2\pi^2 s^2 (\sigma_C^2 + \sigma_A^2)] \exp[2\pi s i (C_0 + A_0)] = \exp(-2\pi^2 s^2 \sigma_L^2) \exp(2\pi s i L_0)$

and: $|F_C| = \exp(-2\pi^2 s^2 \sigma_C^2)$ $|F_A| = \exp(-2\pi^2 s^2 \sigma_A^2)$ $|F_L| = \exp(-2\pi^2 s^2 \sigma_L^2)$

Just two modifications proposed by Blundell [6] have been introduced into the model. The existence of a transition layer at the phase boundaries, with a linear electron density profile across the interface, is taken into account by introducing a term $T(s)$:

$$I_1(s) = I_B(s) \cdot T(s) \quad \text{where } T(s) = \left(\frac{\sin \pi E s}{\pi E s} \right)^2 \quad (8)$$

and E is the thickness of the transition layer.

Additionally, it is assumed [6] that the reduced standard deviations of the crystalline and amorphous layer thickness distributions are equal to each other.

$$\frac{\sigma_C}{C_0} = \frac{\sigma_A}{A_0} = g \quad (9)$$

After such modifications, the final form of the formula for the intensity scattered by a stack [eq. (1)] is:

$$I_1(s) = K \frac{\varphi}{s^2 C_0} \frac{1 - |F_L|^2 - |F_C| \left((1 - |F_A|^2) \cos(2\pi s C_0) - |F_A| \left((1 - |F_C|^2) \cos\left[2\pi s \left[C_0 \frac{1-\varphi}{\varphi} \right] \right) \right) \right)}{1 - 2|F_L| \cos\left[2\pi s \frac{C_0}{\varphi} \right] + |F_L|^2} \cdot T(s) \quad (10)$$

where $C_0/L_0 = \varphi$ is the volume crystallinity of stack, K is the scaling constant and:

$$|F_C| = \exp(-2\pi^2 s^2 g^2 C_0^2) \quad |F_A| = \exp\left(-2\pi^2 s^2 g^2 C_0^2 \left[\frac{1-\varphi}{\varphi} \right]^2\right) \quad |F_L| = \exp\left(-2\pi^2 s^2 g^2 C_0^2 \left[1 + \left(\frac{1-\varphi}{\varphi} \right)^2 \right]\right)$$

In this work, the theoretical intensity function given by eq. (10) was fitted to the experimental curves of investigated polymers. The function has five independent parameters, optimized by best-fitting method: scaling constant K , average thickness of crystalline lamellae C_0 , volume crystallinity of stacks φ , reduced standard deviation g and transition layer thickness E .

VARIABLE LOCAL STRUCTURE MODEL

In this model, the structure of all stacks contained in a polymer volume is not the same, i.e. the polymer is inhomogeneous in terms of the structure of stacks. Such inhomogeneous models and methods of their analysis have already been proposed by Strobl and Muller [11], Stribeck [12, 13] and Blundell [10]. Stribeck elaborated a method based on Ruland's [16] interface distribution function (IDF) which was used in the investigation of PET samples. In this method, the parameters of stacks are determined by best fitting of a theoretical IDF function constructed for investigated polymer, to the experimental IDF calculated from its SAXS curve. The theoretical IDF includes in one analytical expression the paracrystalline

disorder of stacks, their finite size and inhomogeneity by using so called "compansion principle" which is mathematically expressed by Mellin convolution.

In our work a method proposed by Blundell has been adopted. It is assumed that the stacks differ in their volume crystallinity which varies from stack to stack according to some distribution function $P(\varphi)$. For such a case, the total scattered intensity per unit volume of the polymer, is a weighted average of intensities scattered by all stacks of various crystallinity [10]:

$$I_1(s) = \int_0^1 I_1(s, \varphi) P(\varphi) d\varphi \quad (11)$$

where: $I_1(s, \varphi)$ — the intensity from a stack of the volume crystallinity φ , $P(\varphi)$ — a normalized distribution function giving the probability that such stack occurs.

Additionally, to establish the relationship between the local crystallinity and the structure of an individual stack, it is assumed that the average thickness C_0 of crystalline lamellae is the same in all stacks. So, different crystallinity of various stacks means different average thickness of amorphous layers and consequently different long period. Namely, the stacks of higher crystallinity have shorter average long period. Other two parameters assumed as the same in all stacks are: the reduced standard deviations g of the distribution functions $G_1(C)$ and $G_2(A)$ and the thickness E of the transition layer between the phases.

Based on this model, we calculate the theoretical intensity function $I_1(s)$ from the integral (eq. 11) where $I_1(s, \varphi)$ is the basic function of Hosemann, given by eq. (10). So, it is still assumed that the number of lamellae N in a stack is large enough that the zero order component $I_C(s)$ can be neglected and that $G_1(C)$ and $G_2(A)$ are Gauss distributions with the same reduced standard deviation g . The function $I_1(s, \varphi)$ has two variables — s and φ and four parameters: scaling factor K , average thickness of crystalline lamellae C_0 , reduced standard deviation g , and the transition layer thickness E .

The calculations described in this paper were performed for several probability functions $P(\varphi)$. Each of them has two independent parameters. First of them (φ_0 or φ_s) is the mean or the most probable value of φ . The second one (σ , σ_e , γ) expresses the width of a distribution. At first a symmetric Gauss function was assumed:

$$P(\varphi) = \frac{1}{\sigma\sqrt{2\pi}} \exp\left[-\frac{(\varphi - \varphi_0)^2}{2\sigma^2}\right] \quad (12)$$

Next, three asymmetric, functions were tested;

1. Exponential function

$$\begin{aligned} \varphi \leq \varphi_s \quad P(\varphi) &= 0 \\ \varphi > \varphi_s \quad P(\varphi) &= \frac{1}{\sigma_e} \exp\left[-\frac{\varphi - \varphi_s}{\sigma_e}\right] \end{aligned} \quad (13)$$

2. "Half-Gauss" function

$$\begin{aligned} \varphi \leq \varphi_s \quad P(\varphi) &= 0 \\ \varphi > \varphi_s \quad P(\varphi) &= \frac{1}{\sigma\sqrt{2\pi}} \exp\left[-\frac{(\varphi - \varphi_s)^2}{2\sigma^2}\right] \end{aligned} \quad (14)$$

3. Reinhold function [17] (see Fig. 1)

$$\begin{aligned} \varphi \leq \varphi_0(1 - 2\gamma) \quad P(\varphi) &= 0 \\ \varphi > \varphi_0(1 - 2\gamma) \quad P(\varphi) &= \frac{[\varphi - \varphi_0(1 - 2\gamma)]}{(\gamma\varphi_0)^2} \exp\left[-\frac{[\varphi - \varphi_0(1 - 2\gamma)]}{\gamma\varphi_0}\right] \end{aligned} \quad (15)$$

where γ – the reduced standard deviation.

The functions listed above are positively skewed. Apart from them, three similar but negatively skewed function were tried.

It is obvious that in all cases the probability function $P(\varphi)$ must be normalized to unity and that crystallinity must meet a condition: $0 \leq \varphi \leq 1$. Consequently, the integral:

$$\int_0^1 P(\varphi) d\varphi \cong 1 \quad (16)$$

must be equal to 1 or must be very close to 1. It means, that the parameters of the $P(\varphi)$ function are dependent on one another and appropriate constraints must be put on them in numerical calculations.

Figure 2 illustrates how this problem was solved in the case of Gauss function. In this case, the integral (16)

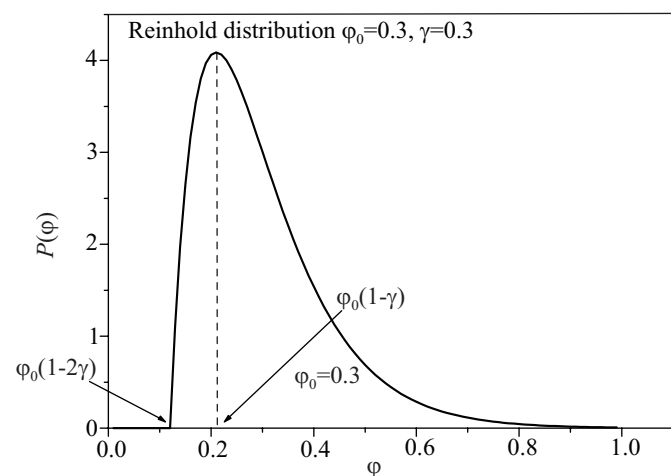


Fig. 1. Reinhold distribution with the mean φ_0 and the width parameter γ (reduced standard deviation) equal to 0.3; maximum is located at 0.21; the function is equal to zero for φ smaller than 0.12

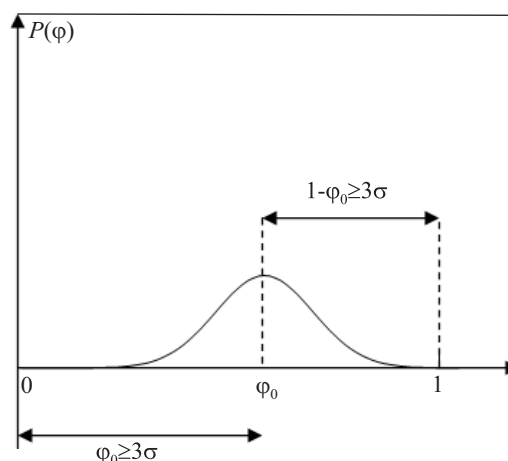


Fig. 2. Constraints put on the mean φ_0 and standard deviation σ of the Gauss distribution to fulfill the normalization condition (16)

amounts to 0.9973. Similar solutions were found for asymmetric functions.

EXPERIMENTAL PART

Materials

Two grades of melt crystallized ethylene-1-octene copolymers produced by DSM Research (The Netherlands) were investigated: copolymer EO5 with 5.5 mol % of 1-octene and copolymer EO6 with 6.6 mol %. The copolymers were synthesized using a metallocene catalyst system.

Methods of testing

SAXS curves were recorded during cooling of the samples from the melt (90 °C and 79 °C respectively) to 25 °C and 21 °C respectively, at a constant rate of 10 °C/min. The samples of a thickness of 1mm and diameter of 5 mm were sealed between thin aluminum foils. During SAXS measurements a sample was placed in the X-ray beam path in a Mettler FP-82HT hot stage. Before the measurements, each sample was kept at the temperature of 150 °C for 5 min to melt it completely and to erase its thermal history. The temperature of the samples was controlled by the hot stage. For the copolymer EO5, the SAXS curves were recorded every 2 °C and their total number amounted to 33 while for the sample EO6 it was 58 curves recorded every 1 °C. Such a relatively big sets of curves, recorded at various temperatures, enabled us to test if the proposed models correctly described the lamellar structure of investigated copolymers at different stages of crystallization.

The time resolved synchrotron measurements were performed at EMBL laboratory of DESY in Hamburg. SAXS curves were recorded in the range of $2.23 \cdot 10^{-3} \text{ \AA}^{-1} < s < 4.45 \cdot 10^{-2} \text{ \AA}^{-1}$. SAXS data processing was preceded by their normalization to the intensity of primary beam and correction for the detector response. Moreover, an avera-

ged melt pattern of a given sample was subtracted from each curve to eliminate the scattering coming from the sample holder.

All calculations were performed with our computer program SAXSDAT [14]. Theoretical intensity functions described by eq. (10) and (11) were best fitted to the experimental curves using new, modified module of the program, elaborated to this aim. The module has been equipped with several $P(\varphi)$ functions mentioned above. The curves were fitted using the classical non-linear optimization procedure of Rosenbrock [18]. Before fitting, the experimental SAXS curves were subject to introductory numerical elaboration. At first a constant background scattering, resulting from the electron density fluctuations within the phases [19, 20], was subtracted from the curves. Next, the experimental curves $I(s)$ were smoothed and transformed into one-dimensional scattering functions I_{1e} by the Lorentz correction [10, 15]:

$$I_{1e}(s) = 4\pi s^2 I(s) \quad (17)$$

As a result of fitting, the parameters of stacks were determined.

Independently, the parameters of stacks were determined from the one-dimensional correlation function which is the Fourier transform of the experimental curve. The correlation functions were calculated and analyzed by means of the SAXSDAT program according to the procedures described in [14], based on the methods developed by Strobl [1] and Vonk [2].

RESULTS AND DISCUSSION

At first, we assumed that the model of Hosemann was suitable to describe the structure of investigated copolymers and we tried to fit the related theoretical intensity function given by eq. (10) to the experimental SAXS curves. However, the quality of fit was very poor for all analyzed curves (Fig. 3).

It should be emphasized that in the calculations we put a constraint limiting the maximum value of the redu-

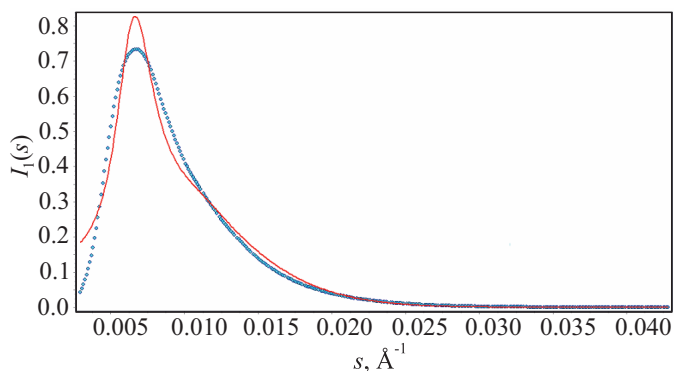


Fig. 3. One-dimensional experimental SAXS curve for the copolymer EO6 at 55 °C (points) and the best fitted theoretical function (solid line), related to the model of Hosemann [eq. (10)]

ced standard deviation g of the thickness distributions $G_1(C)$ and $G_2(A)$: $g \leq 1/3$. This was to minimize unrealistic situations where negative thicknesses of the layers could be admitted. The employed constraint provided the probability of such cases to be less than 0.0027.

The negative result of those trials indicated that the structure of copolymers is more complex than predicted by the model of Hosemann. For this reason it was admitted the possibility that the copolymers are not homogeneous. We assumed the variable local structure model according to which, the volume crystallinity is not the same for all stacks and it varies according to some distribution function $P(\varphi)$. We started with the symmetrical Gauss function, however the quality of fit was only slightly better than the one obtained with the model of Hosemann. This conclusion is consistent with the results obtained by Blundell who investigated the lamellar structure of PE-LD assuming a variable stack model in which the $P(\varphi)$ was a Gauss function. Blundell found that this model gave better fits than obtained with the model of Hosemann, however still imperfect [10]. For this reason, our next trials were performed with asymmetric functions listed above. General conclusion resulting from those trials was that only positively skewed functions give some progress in the quality of fitting. The negatively skewed do not fit completely. It was found that the best quality of

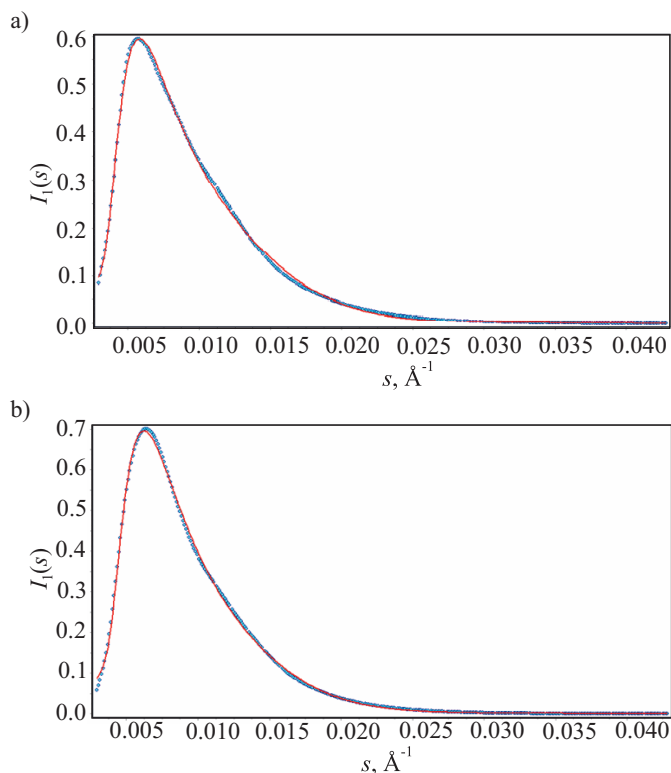


Fig. 4. One dimensional experimental SAXS curve for the copolymer EO6 at: a) 68 °C and b) 58 °C (points) and the best fitted theoretical function (solid line), related to the variable local structure model with the Reinhold function used as crystallinity distribution function $P(\varphi)$

fitting was obtained with the Reinhold function. Two examples are shown in Fig. 4.

As one can see, the theoretical curves are very well fitted in a broad range of scattering angles. Similar quality of fit was obtained for most analyzed curves of both investigated copolymers, recorded at various temperatures. To confirm the correctness of the assumed model, the parameters of stacks obtained from curve fitting method were compared with those ones determined from the correlation function. Such a comparison for the copolymer EO6 is shown in Fig. 5.

One can see that the results obtained with the two methods remain in a very good agreement in a broad range

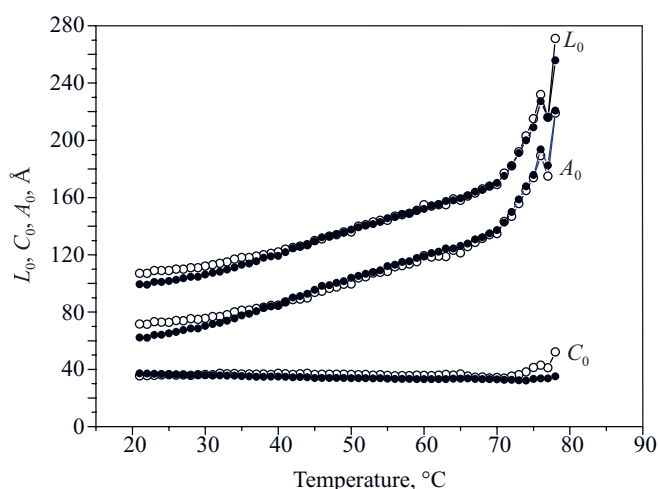


Fig. 5. Average parameters of stacks in the copolymer EO6 during cooling from 79 °C to 21 °C, determined from the correlation function (empty circles) and from the curve fitting method with Reinhold function used as a crystallinity distribution function $P(\varphi)$ (black points)

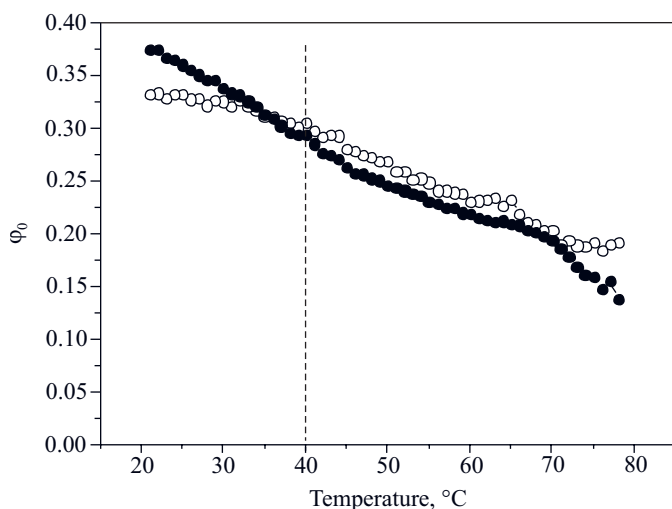


Fig. 6. Average volume crystallinity φ_0 of the copolymer EO6 during cooling from 79 °C to 21 °C, determined from the correlation function (empty circles) and from the curve fitting method with Reinhold function used as a crystallinity distribution function $P(\varphi)$ (black points)

of temperatures. The agreement is very good, but below 40 °C some discrepancies can be observed. Similar discrepancies are visible in the plot of the average volume crystallinity determined with the two methods (Fig. 6).

An analogous behavior was observed in the case of the copolymer EO5; the agreement of the results was very nice at higher temperature, but discrepancies started below about 55 °C.

It is clear, that the Reinhold distribution correctly describes the crystallinity distribution in the stacks at higher temperatures, but at lower temperatures, close to the final solidification, this distribution cease to be appropriate. Such a conclusion is confirmed by inspection of the quality of fitting for the curves recorded below 40 °C (see Fig. 7a and 7b.) — it is already not as good as in the case of curves recorded at higher temperatures.

Seeking for better solution we constructed another asymmetric distribution — a split Gauss function. The split Gauss is a combination of two Gauss functions of various standard deviations on its left and right side:

$$\begin{aligned} \varphi \leq \varphi_s \quad P(\varphi) &= \frac{2}{\sigma\sqrt{2\pi}(n+1)} \exp\left[-\frac{(\varphi - \varphi_s)^2}{2\sigma^2}\right] \\ \varphi > \varphi_s \quad P(\varphi) &= \frac{2}{\sigma\sqrt{2\pi}(n+1)} \exp\left[-\frac{(\varphi - \varphi_s)^2}{2n^2\sigma^2}\right] \end{aligned} \quad (18)$$

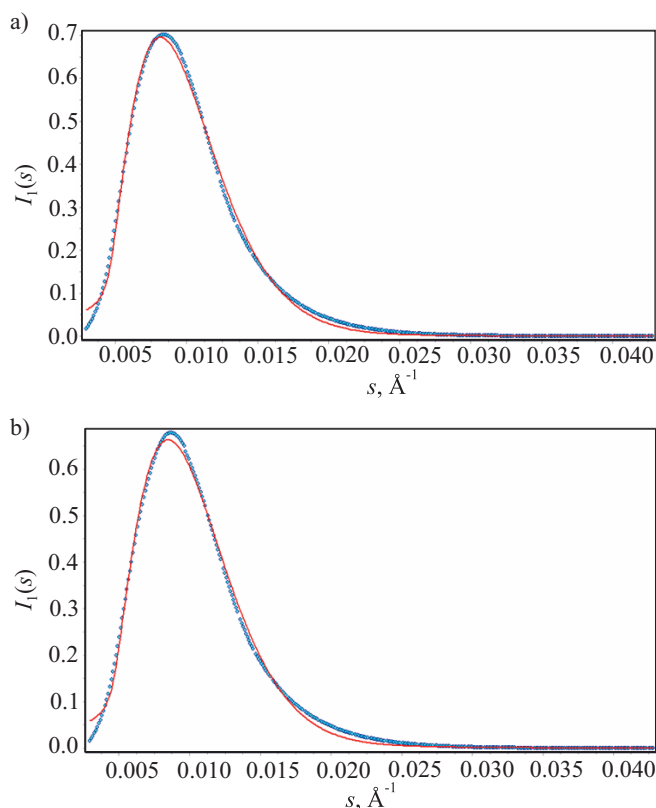


Fig. 7. One-dimensional experimental SAXS curve for the copolymer EO6 at a) 29 °C and b) 21 °C (points) and the best fitted theoretical function (solid line), related to the variable local structure model with the Reinhold function used as crystallinity distribution function $P(\varphi)$

The formula above describes a split Gauss function in which the standard deviation on the right side is n -times larger than that one on the left side. Later on, the coefficient n — will be referred to as the *asymmetry factor*. Similarly as the classical Gauss function, the function (18) is normalized to unity when the limits of integration are infinite. In our calculations, where $0 \leq \varphi \leq 1$, the parameters: σ , n and φ_s were constrained in this way that: $\varphi_s \geq 3\sigma$ and $1-\varphi_s \geq 3n\sigma$. As a result, the integral (16) amounted to 0.9973.

The split Gauss was useful in our work, because changing n we could easily vary the asymmetry of the crystallinity distribution. We tried to take different asymmetry factors and it had turned out that the best results were obtained when it was equal to 9. In the case of the curves recorded at lower temperatures, substitution of the Reinhold function with the split Gauss, results in a good fit of the theoretical and experimental curves and a good

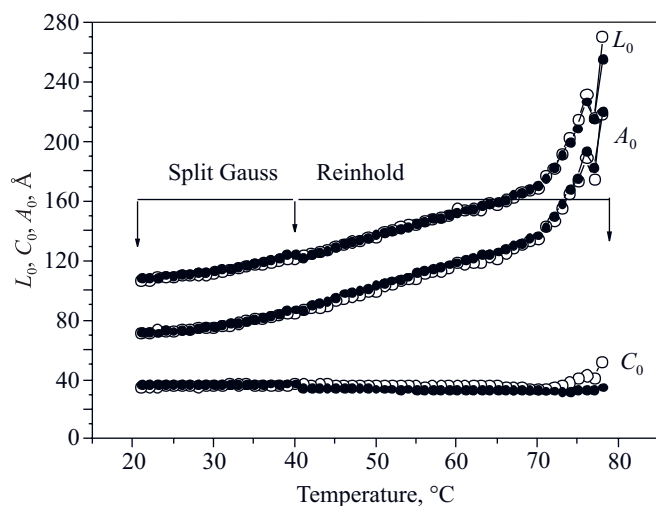


Fig. 8. Average parameters of stacks in the copolymer EO6 during cooling from 79 °C to 21 °C, determined from the correlation function (empty circles) and from the curve fitting method (black points); the temperature ranges in which the split Gauss and Reinhold functions were used as the crystallinity distribution $P(\varphi)$ are indicated

agreement of the parameters values determined from curve fitting method and from correlation function. Such a comparison for the copolymer EO6 is shown in Figs. 8 and 9.

Similarly good agreement was obtained for the sample EO5.

In Fig. 10 we see the split Gauss function and the Reinhold function found for the SAXS curve recorded at $t = 25$ °C i.e. at the temperature for which the Reinhold function does not provide a good fit (see Figs. 5 and 6). The parameters of these functions shown in the figure were determined with curve-fitting method. As it results from this comparison, at low temperatures the shape of the crystallinity distribution is still asymmetric but it beco-

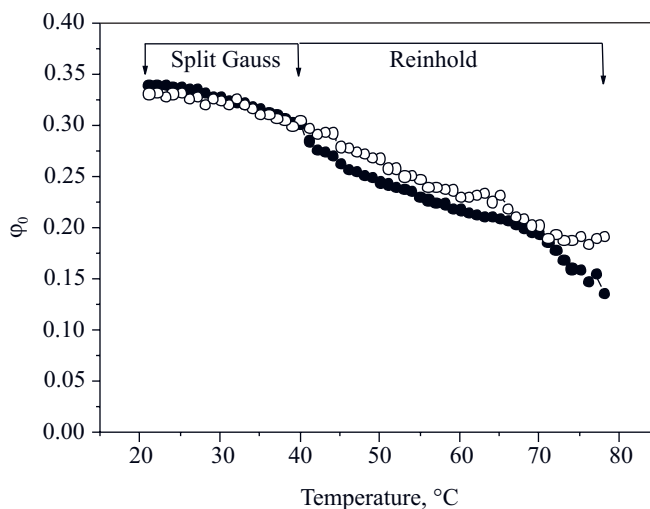


Fig. 9. Average volume crystallinity φ_0 of the copolymer EO6 during cooling from 79 °C to 21 °C, determined from the correlation function (empty circles) and from the curve fitting method (black points); the temperature ranges in which the split Gauss and Reinhold functions were used as the crystallinity distribution $P(\varphi)$ are indicated

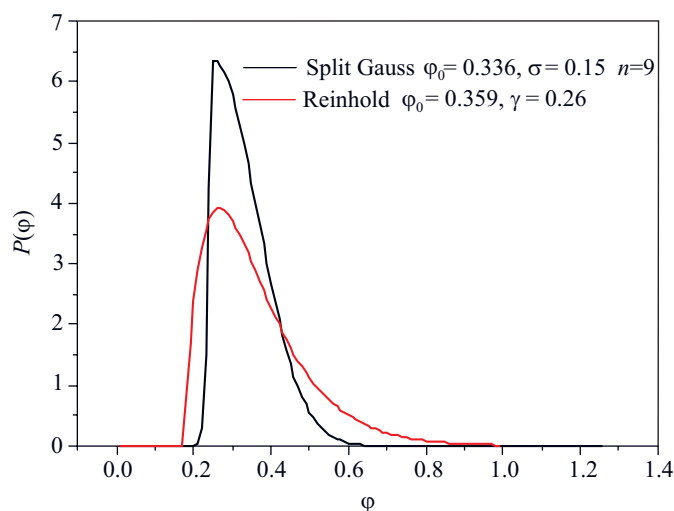


Fig. 10. A comparison of the split Gauss function with the asymmetry factor $n = 9$ (black), and Reinhold function (red) for the SAXS curve recorded at $t = 25$ °C; the parameters of these functions found by optimization procedure are given in the figure

mes more compact than that one of the Reinhold function.

CONCLUSIONS

This work aimed at modeling of the lamellar structure of ethylene-1-octene copolymers of moderate (5.5 mol % and 6.6 mol %) concentration of 1-octene. It was shown that the general model of Hosemann [5] and theoretical intensity function based on this model [eq. (10)] are not appropriate for this copolymers. Performed investigations indicate that differently to what is assumed in the model of Hosemann, the copolymers are not homogene-

ous in terms of the structure stacks: the volume crystallinity is not the same for all stacks and it varies according to some distribution function $P(\varphi)$. In other words the variable local crystallinity model is more realistic. Similarly as Blundell found for PE-LD [10], we observed that the variable crystallinity model in which $P(\varphi)$ is a Gauss distribution gave better fits than the model of Hosemann but they are still considerably imperfect. We have shown that generally, the distribution function is asymmetric and positively skewed but its shape changes for the stacks crystallized at various temperatures. At higher temperatures, starting from the melting point, the crystallinity distribution can be well approximated by the Reinhold function. However at lower temperatures, close to the final solidifications, the split Gauss function with the asymmetry factor of 9 is a better approximation.

Most probably, the inhomogeneity of the lamellar structure of investigated copolymers results from the phenomenon of molecular segregation. In the investigated ethylene-1-octene copolymers, the 1-octene comonomers form short hexyl branches which are randomly distributed along the main polyethylene chain. These side branches disrupt the regularity of the main chain and divide it into ethylene sequences of different lengths which are able to crystallize. Obviously, the kinetics of crystallization and the morphology of crystals originating during solidification depends on the sequence length distribution. During crystallization, the longer sequences crystallize first forming stacks of higher crystallinity. Next, the sequences of the most probable length form the major number of stacks. The shortest sequences do not crystallize at all being incorporated into the amorphous phase.

Our result on the asymmetric, positively skewed shape of the crystallinity distribution $P(\varphi)$ in stacks agree with the conclusion stated by Stribeck for PET samples [12, 13]. Stribeck found that the asymmetry of the distribution of long periods in stacks and of the global distributions of the thicknesses of crystalline and amorphous layers resulted directly from the "compansion principle" that he introduced (which was mathematically expressed by the Mellin convolution). On the other hand some researchers e.g. [7, 8] report that they have obtained reliable results (i.e. good fits to experimental curves) assuming that the structure of all stacks is statistically identical and using the classical model of Hosemann for investigated polymers or assuming a symmetrical Gauss distribution of crystallinity in stacks [9]. These facts suggest that it is

difficult to formulate some general conclusions on the homogeneity or inhomogeneity of stacks in a given polymer sample. Most probably it is dependent on several factors from among which the type of a polymer and its thermal history seem to be the most important.

REFERENCES

- [1] Vonk C.G, Kortleve G.: *Kolloid Z. Z. Polym.* **1967**, 220, 19.
- [2] Strobl G.R., Schneider M.: *J. Polym. Sci., Polym. Phys. Ed.* **1980**, 18, 1343, <http://dx.doi.org/10.1002/pol.1980.180180614>
- [3] Crist B.: *J. Polym. Sci. Polym. Phys. Ed.* **1973**, 11, 635.
- [4] Stribeck N.: „X-Ray Scattering of Soft Matter“, Springer-Verlag, Berlin Heidelberg 2007, <http://dx.doi.org/10.1007/978-3-540-69856-2>
- [5] Hosemann R., Bagchi S.N.: „Direct Analysis of Diffraction by Matter“, North Holland, Amsterdam 1962.
- [6] Blundell D.J.: *Acta Cryst.* **1970**, A26, 476, [http:// dx.doi.org/10.1107/S0567739470001262](http://dx.doi.org/10.1107/S0567739470001262)
- [7] Isoda S., Shimada H., Kochi M., Kambe H.: *J. Polym. Sci., Polym. Phys. Ed.* **1981**, 19, 1293, <http://dx.doi.org/10.1002/pol.1981.180190902>
- [8] Kochi M., Kambe H.: *Polym. Eng. Rev.* **1983**, 3, 355.
- [9] Marenga C., Marigo A., Cingano G., Zanetti R.: *Polymer* **1996**, 37, 5549, [http://dx.doi.org/10.1016/S0032-3861\(96\)80440-X](http://dx.doi.org/10.1016/S0032-3861(96)80440-X)
- [10] Blundell D.J.: *Polymer* **1978**, 19, 1258, [http://dx.doi.org/10.1016/0032-3861\(78\)90302-6](http://dx.doi.org/10.1016/0032-3861(78)90302-6)
- [11] Strobl G.R., Muller N.J.: *J. Polym. Sci.* **1973**, 11, 1219.
- [12] Stribeck N.: *Colloid Polym. Sci.* **1993**, 271, 1007, [http:// dx.doi.org/10.1007/BF00659290](http://dx.doi.org/10.1007/BF00659290)
- [13] Stribeck N.: *J. Phys. IV* **1993**, 3(C8), 507, <http://dx.doi.org/10.1051/jp4:19938105>
- [14] Rabiej S., Rabiej M.: *Polimery* **2011**, 56, 662.
- [15] Crist B.: *J. Macromol. Sci. Phys.* **2000**, B39, 493, [http:// dx.doi.org/10.1081/MB-100100401](http://dx.doi.org/10.1081/MB-100100401)
- [16] Ruland W.: *Colloid Polym. Sci.* **1977**, 255, 417, [http:// dx.doi.org/10.1007/BF01536457](http://dx.doi.org/10.1007/BF01536457)
- [17] Reinhold C., Fischer E.W., Peterlin A.: *J. Appl. Phys.* **1964**, 35, 71, <http://dx.doi.org/10.1063/1.1713101>
- [18] Rosenbrock H.H., Storey C.: „Computational Techniques for Chemical Engineers“, Pergamon Press, Oxford 1966.
- [19] Ruland W.: *J. Appl. Crystallogr.* **1971**, 4, 70, <http://dx.doi.org/10.1107/S0021889871006265>
- [20] Koberstein J. T., Morra B., Stein R. S.: *J. Appl. Crystallogr.* **1980**, 13, 34, <http://dx.doi.org/10.1107/S0021889880011478>